Abrupt change in North African hydroclimate and landscape evolution 3.2 million years ago

Katharine Grant (katharine.grant@anu.edu.au)
The Australian National University https://orcid.org/0000-0003-4299-5504

Udara Amarathunga
Australian National University https://orcid.org/0000-0002-9743-0677

Jessica Amies
The Australian National University https://orcid.org/0000-0002-8282-9175

Pengxiang Hu
Australian National University

Yao Qian
Australian National University

Tiah Penny
Australian National University

Laura Rodríguez-Sanz
The Australian National University

Xiang Zhao
Australian National University

David Heslop
The Australian National University

Diederik Liebrand
MARUM https://orcid.org/0000-0002-6925-7889

Rick Hennekam
Royal Netherlands Institute for Sea Research https://orcid.org/0000-0002-8823-4519

Thomas Westerhold
MARUM - University Bremen https://orcid.org/0000-0001-8151-4684

Stewart Gilmore
Geoscience Australia

Lucas Lourens
Faculty of Geosciences, Utrecht University

Andrew Roberts
Australian National University https://orcid.org/0000-0003-0566-8117

Eelco J Rohling
Australian National University https://orcid.org/0000-0001-5349-2158

Article

Keywords: North African hydroclimate, landscape evolution, dark organic-rich layers (sapropels)

Posted Date: June 21st, 2021

DOI: https://doi.org/10.21203/rs.3.rs-579142/v1

Abrupt change in North African hydroclimate and landscape evolution 3.2 million years ago

K.M. Grant[1*], U. Amarathunga[1], J.D. Amies[1], P.X. Hu[1], Y. Qian[1], T. Penny[1], L. Rodriguez-Sanz[1], X. Zhao[1], D. Heslop[1], D. Liebrand[2]†, R. Hennekam[3], T. Westerhold[2], S. Gilmore[5], L.J. Lourens[4], A.P. Roberts[1], E.J. Rohling[1,6]

[1] Research School of Earth Sciences, Australian National University, ACT 2601, Canberra, Australia
[2] MARUM, University of Bremen, D-28359 Bremen, Germany
[3] NIOZ Royal Netherlands Institute for Sea Research, Department of Ocean Systems, P.O. Box 59, 1790 AB, Den Burg, Texel, the Netherlands
[4] Department of Earth Sciences, University of Utrecht, Utrecht 3584 CD, The Netherlands
[5] Geoscience Australia, GPO Box 378, ACT 2609, Canberra, Australia
[6] Ocean and Earth Science, University of Southampton, National Oceanography Centre, Southampton, SO14 3ZH, UK
† Now at PalaeoClimate.Science, Allerton Bywater, United Kingdom

* Correspondence to: katharine.grant@anu.edu.au

Dark organic-rich layers (sapropels) have accumulated in Mediterranean sediments since the Miocene due to deep-sea dysoxia and enhanced carbon burial at times of intensified North African run-off during 'Green' Sahara Periods (GSPs). The existence of orbital precession-dominated Saharan aridity/humidity cycles is well known, but lack of long-term, high-resolution records hinders understanding of their precise relationships with environmental and hominin evolution. Here we present continuous, high-resolution geochemical and environmental magnetic records for the Eastern Mediterranean that span the past 5.2 million years, which reveal that organic burial in sapropels intensified 3.2 Myr ago. We deduce that fluvial terrigenous sediment inputs during GSPs doubled abruptly at this time, whereas monsoon run-off intensity remained relatively constant. We attribute the increase in sediment mobilisation to an abrupt non-linear North African landscape response associated with a major increase in arid:humid contrasts between GSPs and intervening dry periods. This likely limited hominin (and other animal) inhabitation of, and migration through, the Sahara region to GSPs only.

'Green Sahara Periods' (GSPs) have been a fundamental characteristic of North African climate change for more than 8 Ma[ref.1]. Only the most recent GSP during the early-mid Holocene (~11 to 6 thousand years ago, ka; the 'African Humid Period') has been studied in detail at numerous locations[2-4], and it extended to East Africa[5-7]. However, there are

few continuous, well-dated records of GSPs that extend beyond the Pleistocene (or beyond the last 300 ka), and no high-resolution North African humidity reconstructions encompass the entire Plio-Pleistocene. Mediterranean sediments contain a particularly rich archive of past GSPs. Here, organic-rich layers ('sapropels') form in response to deep-sea anoxia and nutrient inputs when significantly increased run-off enters the basin via the Nile and wider North African margin[8]. These periods correspond to enhanced boreal summer insolation maxima and minima in Earth's orbital precession cycle, resulting in a more northerly and intensified African rainbelt[8,9]. Sapropels are a natural testbed for understanding deep-sea redox and carbon burial processes; however, their formation mechanisms are still debated[8], and there is currently no continuous high-resolution proxy record of Plio-Pleistocene sapropels.

Ba/Al, Ti/Al, and planktic $\delta^{18}O$ in Eastern Mediterranean sediments are useful proxies of past GSPs and sapropels. Ba/Al reliably tracks sapropel intervals because it correlates with original organic carbon burial (C_{org}) in sapropels and is mostly unaffected by post-depositional redox reactions[10], while surface water freshening due to monsoon run-off is recorded by strong negative $\delta^{18}O$ peaks[11,12]. Ti/Al in the open Eastern Mediterranean reflects relative variations in North African aeolian *vs* riverine inputs to the basin[13]. Both elements are supplied within clays, but aeolian-sourced Ti in the open Eastern Mediterranean is enhanced relative to fluvially-sourced Ti because heavier (Ti-bearing) suspended particles preferentially settle near the Nile fan. Al normalisation (for Ti and Ba) removes clay dilution effects.

Here, we address the dual need for high-resolution records of North African humidity/aridity changes and sapropel deposition through the entire Plio-Pleistocene, by presenting the first continuous, astronomically dated GSP and sapropel proxy records back to 5.2 Ma from Eastern Mediterranean Ocean Drilling Program (ODP) Site 967 (Figures 1-2; Supplementary Figure S1). From the same site, we also present high-resolution records of Saharan dust and riverine inputs over the past 5.2 Ma. Our data reveal a fundamental change in sapropel development, provide much-needed context for understanding hominin evolution and migrations out of Africa, and are essential for modelling the mid-Pliocene—the most recent interval with CO_2 levels approximating modern levels[14].

Green Sahara Periods

Ti/Al, Ba/Al, and planktic $\delta^{18}O$ record GSP timings over the Plio-Pleistocene (Fig. 3). The Ba/Al signal is consistent with a typical sapropel sequence[10,15], and lower Ti/Al values correspond to Ba/Al spikes, $\delta^{18}O$ minima, and precession minima. The $\delta^{18}O$ record reflects long-term global sea level/ice volume changes[16], with superimposed negative $\delta^{18}O$ excursions that relate to African run-off into the Eastern Mediterranean and warming within fresher surface-water layers[12,17,18]. African run-off reaching ODP967 would have derived primarily from the Nile[18,19], which is fed by East African precipitation influenced by both the Indian and African Monsoons and their moisture convergence at the Congo Air Boundary[20]. African run-off also entered the Eastern Mediterranean from the wider North African margin when the African rainbelt migrated northward[18,21,22]. This rainbelt is associated with the intertropical convergence zone (ITCZ), the West African monsoon (WAM), and East African precipitation[20,23]. Thus, ODP967 $\delta^{18}O$ reflects both WAM and East African precipitation. While changes in local Eastern Mediterranean precipitation over the entire Plio-Pleistocene are not well-constrained, their impacts on ODP967 $\delta^{18}O$ are likely to be minimal compared to African run-off because Eastern Mediterranean surface waters are the evaporative source for local precipitation (with little excess $\delta^{18}O$ fractionation)[8,12]. The similar range of $\delta^{18}O$ minima at precession minima throughout the record (Fig. 3, note by convention reversed $\delta^{18}O$ axis) suggests that maximum African (monsoon) run-off into the Eastern Mediterranean reached roughly similar intensities throughout the Plio-Pleistocene. Furthermore, the ODP967 Ba/Al, Ti/Al, and $\delta^{18}O$ records all attest to continuity of run-off maxima and 'sapropel-like' Pliocene C_{org} fluxes.

The longest continuous (albeit low-resolution) time-series of Saharan/North African hydroclimate changes extend back to ~4-4.5 Ma and are based on terrigenous (=non-biogenic) sediment fluxes offshore of Northwest Africa and Arabia[24,25], where terrigenous components are primarily sourced from aeolian dust[25]. At ODP967, an isothermal remanent magnetization (IRM) proxy for hematite ($IRM_{900@120mT}$; see Methods) reflects Saharan dust inputs to this site[26]. $IRM_{900@120mT}$ values remain relatively low until ~1.4 Ma, with notable increases at 1.2 and 0.9 Ma, coincident with the Mid-Pleistocene transition (MPT) (Fig. 4e). Increased dust fluxes at the MPT are also observed in a lower

resolution ODP967 IRM record extending back to 3 Ma[ref.26,27], and in dust records from ODP sites 664 (Fig. 4h) and 721/722 (Arabian Sea)[27]. There are also discrepancies among these records, and among terrigenous (dust) records from other ODP sites off Northwest Africa[25,27] (Fig. 1). For example, sites more proximal to the Sahara (e.g. ODP659) have high-amplitude dust fluxes throughout the Plio-Pleistocene[25], whereas more distal sites (e.g., ODP662/3 and 664) record higher-amplitude dust fluxes from ~3 Ma and 2.7 Ma (Fig. 4g,h). At ODP Site 959, Ti/Al values suggest increasing aeolian dust inputs from ~3.5 Ma, with potentially a slight increase at 3.2 Ma (Fig. 4i), although the record may partly reflect Guinea Current changes[28]. Lower dust inputs tend to coincide with GSPs, but not consistently (Supplementary Figure S3); instead, they likely relate to distance from dust source areas and prevailing dust trajectories[25,27], i.e., factors other than humidity/aridity changes.

The Plio-Pleistocene sapropel record

Intriguingly, there are no visibly preserved sapropels in most of the Pliocene portion of ODP967[ref.29] (Fig. 2) – visible sapropels appear from 3.2 Ma onward. However, not all Eastern Mediterranean ODP sites record the same lithological change at 3.2 Ma (Table 1): Sites 964 and 967 lack visible sapropels prior to this time, while Sites 966 and 969 contain a continuous visible sapropel sequence down to the core base at 4.5 and 5.3 Ma, respectively[29]. This difference remains unexplained. It is unlikely to relate to Pliocene sedimentation rates which are similar among the four sites (Supplementary Fig. S4), but may relate to water depth, because Pliocene sapropels are absent from the deepest sites[29]. Spatial offsets in the timing, duration, and intensity of sapropel formation are expected[8,30], but such a dramatic contrast in Pliocene sapropel preservation among Eastern Mediterranean sites implies basin-wide changes in the balance of deep-water oxygen supply (ventilation) *vs* demand (C_{org} remineralization and, likely, export).

The ODP967 sapropel-sequence change coincides with a shift to larger amplitude Ba/Al and Ti/Al fluctuations (Fig. 4b-d), a two-to-threefold increase in terrigenous element concentrations (Supplementary Fig. S5), and a shift in the mean and variance of Ti/Al based on change-point analysis (Fig. 4c). Elevated terrigenous element concentrations at ODP967 (Supplementary Fig. S5) are associated with insolation maxima, in line with their primarily riverine transport via the Nile and wider North African margin[19,22,31]. In

contrast, ODP967 element fluxes reflect sediment density changes associated with sapropel lithology (Supplementary Fig. S6); hence, relative variations in terrigenous *versus* biogenic element concentrations more accurately indicate terrigenous inputs. The 3.2 Ma geochemical shift and sapropel deposition/preservation change thus implies a major increase in monsoon run-off and/or suspended load, or a fundamental reorganization of Eastern Mediterranean deep-water circulation and sedimentation. We formulate four testable hypotheses (Table 2) that invoke: a) a marked change in North African climate/landscape (Hypotheses 1-2; $H_{1,2}$); and b) Sicily Sill uplift ($H_{3,4}$). We now consider our results in the context of these scenarios.

African climate/environment shift at 3.2 Ma

Considering H_1 (see Table 2), a marked increase in freshwater run-off into the Eastern Mediterranean would be registered in ODP967 $\delta^{18}O$, irrespective of the freshwater source. However, ODP967 $\delta^{18}O$ reaches similar minima throughout the last 4.5 Ma (Fig. 3). H_1 also implies a shift to more rainfall after 3.2 Ma, which is inconsistent with pollen data[32] (Fig. 4f) and modelling results[33-35] that indicate a generally greener Pliocene Sahara (i.e., forests and wetlands). Leaf wax $\delta^{13}C_{31}$ at ODP Site 659 (Fig. 1) is generally more negative in the Pliocene compared with the last glacial cycle, which is consistent with elevated Pliocene North African humidity[36]. Similarly in Northeast Africa, high-resolution pollen and tree index records from the Baringo Basin reveal a marked shift to drier conditions at 3.2 Ma[ref.37] (Fig. 4j), which is consistent with leaf wax isotope data from DSDP Site 231 in the Gulf of Aden[38] (Fig. 4k). Leaf wax isotope records (δD, $\delta^{13}C$) in that study were interpreted in combination with other regional palaeoclimate records, and suggest two main shifts to drier conditions: at 5-4.5 and 3.3-3.0 Ma. Hence, available evidence causes us to reject H_1.

H_2 implies a more erodible North African landscape from ~3.2 Ma onward, which in turn suggests more arid or variable climate conditions, or the emergence of new—possibly seasonal—drainage pathways. Equally, a reduction in soil-stabilizing vegetation would facilitate sediment erosion through existing channels. Pollen records support a shift to increased aridity and climate variability after 3.2 Ma (see above), while dust records are more equivocal: only two ODP sites (662/3 and 664) record a shift to higher amplitude dust inputs at around 3 Ma (Fig. 4g,h). However, aeolian dust records can reflect other

153 factors (e.g., wind patterns, distance to dust source), which could explain some offsets
154 (Sites 662/3 and 664 are more distal from the Sahara than Site 659). Furthermore, if the
155 amplitude increase in ODP967 Ti/Al variations (aeolian *vs* riverine proxy) at 3.2 Ma is
156 African-climate driven, then the lack of a coeval shift in ODP967 $IRM_{900@120mT}$ (aeolian
157 proxy) implies that the Ti/Al change primarily reflects a change in riverine rather than
158 aeolian components. At ODP967, this component is sourced primarily from the Nile[18,19].
159 While the Sahara has likely existed since the Miocene[39], the Nile evolved though the Plio-
160 Pleistocene[40-42]. The timings of its various development stages are not well constrained,
161 but a recent synthesis[41] proposes a Late Pliocene/early Pleistocene connection of the
162 Blue Nile/Atbara-Tekeze rivers to the palaeo-Nile, and emergence of the modern
163 Egyptian Nile flood plain and delta (the White Nile joined the main channel within the last
164 0.5 Ma[ref.41]). Nile evolution could, therefore, account for a major mid/late Pliocene shift
165 in drainage pathways and suspended sediment.
166
167 It is implicit to H_2 (and inferred from our ODP967 $\delta^{18}O$ record) that freshwater run-off
168 fluxes during GSPs must have been decoupled from long-term changes in suspended
169 sediment loads. Several lines of evidence suggest that this is plausible. First, factors
170 determining river sediment loads over geological time reflect a complex interplay of
171 tectonics (e.g., rock type, relief) and climate (e.g., precipitation, run-off). Peak suspended
172 load does not always correspond to peak run-off, unlike typical annual cycles, so
173 landscape changes driven by tectonic (and climate) evolution can result in more erodible
174 surfaces, and thus increased sediment loads, without an attendant change in local
175 rainfall[43]. Second, ecological modelling and data suggest that African biomes are highly
176 sensitive to small reductions in precipitation[44]. Major biome changes in tropical Africa
177 have been simulated without a total annual precipitation change, simply by altering
178 rainfall seasonality[45]. Moreover, inclusion of soil feedbacks in GSP simulations can
179 reproduce pollen-inferred vegetation shifts at around 400mm/yr mean precipitation,
180 relative to ~600 mm/yr in the absence of soil feedbacks[46].
181
182 We also cannot ignore potential effects of large-scale global changes ca 3.2 Ma. The first
183 major Northern Hemisphere glaciation (based on global benthic $\delta^{18}O$) is in stages M2–
184 MG2 at 3.295–3.340 Ma[ref.47] (Fig. 2 and 4n), although the onset was spatially variable and
185 as early as 3.6 Ma[ref.48]. However, the average time-dependent standard deviation of

benthic $\delta^{18}O$ from 25 high-resolution records starts to increase at 3.2 Ma[ref.48]. Stronger high-latitude cooling and intra- and inter-hemispheric SST gradients are observed from ~3.3 Ma[ref.49,50], coeval with a tenfold IRD (ice-rafted debris) flux increase off East Antarctica[51] (Fig. 4m). Central Asian aridification has also been dated to 3.3 Ma, based on halite content, grain size, and magnetic proxies from the Qaidam Basin[52]. All of these developments would have impacted atmospheric dynamics and latitudinal temperature gradients that drive seasonal North African climate variability; we therefore retain *H_2* as a possibility.

Strait of Sicily reconfiguration

Considering *H_3* and *H_4* (Table 2), Mediterranean tectonics could alter basin and sill depths, which would in turn affect deep-water ventilation. Tectonics within the wider Eastern Mediterranean catchment could also affect terrigenous fluxes to the seafloor, by rerouting transportation pathways and/or facilitating more continental erosion. The Mediterranean Basin has been tectonically active since reaching its modern configuration in the Oligocene-Miocene[53]. Detailed palaeomagnetic work on Pliocene sections from Sicily suggests a rapid (80,000-100,000 yrs) differential clockwise rotation at 3.21 Ma, near the C2An.2n-C2An.2r boundary[54] (Fig. 4a). The rotation compressed the Sicilian fold-and-thrust belt and its foreland[54-56] and accelerated Tyrrhenian Sea opening between 3.5 and 2 Ma[ref.54], and is consistent with evidence of middle Pliocene tectonics in the Sicilian Strait[56]. The timing corresponds with the Trubi-Narbonne Formation boundary and may correspond with a rotational phase in northern Italy and a tectonic event north of Crete[54].

The close timing between lithological changes at ODP967 (and likely also at Site 964[ref.29]) and inferred tectonic adjustment of the Sicilian Strait is tantalizing. In the modern Mediterranean, Eastern Mediterranean deep-water flushing over the Sicily sill depends on Bernoulli aspiration (akin to 'pulling' waters out of the eastern basin) and Eastern Mediterranean deep-water formation 'pushing' deep waters out[8]. At the present sill depth (440 m), Bernoulli aspiration is limited to <800 m; deep Eastern Mediterranean ventilation therefore relies on the deep-water formation pump. During sapropel phases, this pump was effectively turned off, leading to anoxic deep waters[8]. Calculations suggest that a 200-400 m deeper Sicily Sill would only marginally affect deep Eastern

Mediterranean ventilation (Methods); nevertheless, we retain *H3* and *H4* for further evaluation.

Deep-sea ventilation *versus* carbon export

Reduced deep Eastern Mediterranean ventilation during sapropel/monsoon periods is forced by surface buoyancy gain (i.e. freshening), yet the relationship between sapropel C_{org} content and degree of buoyancy forcing is complex[8]. Sapropel C_{org} is typically of marine origin, but the type, mechanism, and amount of primary/export production is uncertain; however, consensus suggests a well-developed deep chlorophyll maximum for most sapropels[8]. If increased terrigenous fluxes from 3.2 Ma onward (e.g. hypothesis *H2*) brought more labile terrestrial C_{org} and nutrients to the Eastern Mediterranean, they may have fuelled higher primary productivity and C_{org} export rates relative to the Pliocene, leading to more intensely developed sapropels. Evidence to support/refute this is equivocal or non-existent. Riverine nutrient inputs remain unquantified even for the most recent sapropel[57]. Pliocene sapropels in astronomically dated sections from Sicily and Cyprus contain lower C_{org} concentrations than typical Pleistocene sapropels[58,59], but sapropels in outcrops typically contain less C_{org} and total N than sapropels in offshore cores[60]. There is a general consensus among earlier studies[60-62] that Pliocene and Pleistocene sapropels are similar, and that Pliocene sapropels can contain high C_{org} (≤30%)[ref.62], but the down-core depth intervals studied in these examples correspond to ages younger than 3.1 Ma. Meanwhile, similar early/mid-Pliocene and Pleistocene abundances of *Florisphaera profunda*—indicative of a deep chlorophyll maximum—are observed in sapropels from outcrops in Cyprus[59] and at ODP967[ref.63], implying similarly elevated Pliocene and Pleistocene primary productivity during sapropel deposition.

Nonetheless, hypothesis *H2* cannot account for Eastern Mediterranean ventilation changes after 3.2 Ma, so improved sapropel preservation after 3.2 Ma must be solely due to increased C_{org} export. In contrast, Sicilian Strait shoaling (*H3-4*) could, in principle, induce an increased tendency toward Eastern Mediterranean deep-water stagnation, but—as yet—the evidence remains circumstantial and sparse. Major benthic foraminiferal turnovers are documented between 3.6 and 2.6 Ma in the Punta Piccola section[60] (Southern Italy) and deep ODP sites in the Western and Eastern Mediterranean basins[61], which indicate increasing instability in bottom-water conditions. However, the

main change is focussed at ~2.7 Ma, some 500,000 years after the events discussed here. Coupled Mg/Ca-$\delta^{18}O$ and εNd trends suggest that Mediterranean Outflow Water (MOW) intensified between 3.5 and 3.3 Ma[ref.62], but this pre-dates our observed geochemical shift. Nevertheless, seismic data and drill-core sediments from the Gulf of Cadiz (Fig. 1) indicate a hiatus ca 3.2-3.0 Ma and subsequent contourite deposition, which is attributed to MOW intensification in response to Strait of Gibraltar tectonics[63]. The timing is based on shipboard biostratigraphy, but may be older (~3.4-3.3 Ma) according to a revised mid-late Pliocene chronology for Site U1387[ref.64]. Regardless, deep-water exchange through the Sicilian Strait, rather than the Strait of Gibraltar, is the critical factor for deep ventilation of the Eastern basin[8]. Contributions to Pliocene buoyancy forcing from local precipitation/evaporation are unknown, but we assume that they were negligible relative to African run-off forcing. Likewise, elevated SSTs cannot solely account for buoyancy forcing, given that they only partially contribute to water-column stratification during Last Interglacial sapropel formation[17,18], and mostly in response to salinity-driven stratification.

Mid-Late Pliocene climate and landscape evolution

We have evaluated different hypotheses (climatic *vs* tectonic) to explain a marked shift in Eastern Mediterranean sediments 3.2 Ma ago. We find that sill tectonics ($H_{3,4}$) could account for reduced ventilation after 3.2 Ma (which best explains subsequently increased ODP967 Ba and S concentrations), and may coincide with inferred tectonic activity in the Strait of Gibraltar. However, hypothesis H_3 cannot satisfactorily account for a doubling (or more) of terrigenous element concentrations at ODP967 after 3.2 Ma. Hypothesis H_4 might account for this if the terrigenous influx was locally sourced (i.e., Eastern Mediterranean borderlands), but circumstantial evidence is lacking, and—more importantly—Pleistocene terrigenous sediments at ODP967 predominantly originated from North Africa[19]. Conversely, a non-linear response of riverine terrigenous loads to African climate/landscape evolution (hypothesis H_2) better accounts for increased ODP967 terrigenous element concentrations and Ti/Al fluxes after 3.2 Ma. H_2 can also be directly linked to mid-late Pliocene global climate evolution. Indeed, the 3.2 Ma shift could represent a critical transition in North African landscape in response to a global climate state-shift to icehouse conditions[69]. Increased geochemical signal variance is common prior to critical transitions in Eastern Mediterranean sediments[70], and the biggest

285 systematic Ti/Al variance increase is from 3.4 to 3.2 Ma (Fig. 4d). African pollen evidence
286 attests to a more arid Pleistocene compared to the Pliocene[32,71], and a significantly more
287 erodible landscape must exist before a stepwise amplitude increase in fluvial suspended
288 sediment can occur. Furthermore, North African desert-soil albedo and vegetation
289 feedbacks strongly amplify rainfall variability[46,72,73]. The 3.2 Ma increase in ODP967 Ti/Al
290 and fluvial-sourced terrigenous elements might, therefore, signify the onset of modern-
291 day North African aridity. Nevertheless, we cannot (yet) fully reject H_4. It is conceivable
292 that both H_2 and H_4 are valid and are coupled to major global climatic and tectonic
293 changes; future model-data comparisons should test this.

Acknowledgments

This work was supported by the Australian Research Council grants DE190100042 (KMG), DP190100874 (APR), DP2000101157 and FL1201000050 (EJR), and the Australia-New Zealand IODP Consortium (ANZIC) Legacy/Special Analytical Funding grant LE160100067 (KMG, LRS).

Contributions

KMG designed and led the study and write-up; KMG, UA, JA, TP, YQ and LRS generated $\delta^{18}O$ and magnetism data; DH, PXH and XZ assisted with magnetism measurements; DL performed XRF core-scanning; DL and TW developed the ODP967 composite depth splice and chronology; KMG and RH calibrated scanning XRF data; KMG and SG performed WD-XRF analyses; LL contributed WD-XRF data; all authors contributed to manuscript development.

Ethics declarations

The authors declare no competing interests.

References

1. Larrasoaña, J.C., Roberts, A.P., Rohling, E.J. Dynamics of green Sahara periods and their role in hominin evolution. *PLoS One* 8 (10), e76514. http://dx.doi.org/10.1371/journal.pone.0076514 (2013).
2. Ritchie, J.C., Eyles, C.H., Haynes, C.V. Sediment and pollen evidence for an early to mid-Holocene humid period in the eastern Sahara. *Nature* 314, 352-355 (1985).
3. Drake, N.A., Blench, R.M., Armitage, S.J., Bristow, C.S., White, K.H. Ancient water courses and biogeography of the Sahara explain the peopling of the desert. *Proc. Natl. Acad. Sci. U.S.A.* 108, 458e462. http://dx.doi.org/10.1073/pnas.1012231108 (2010).
4. Shanahan, T.M., McKay, N.P., Hughen, K.A., Overpeck, J.T., Otto-Bliesner, B., Heil, C.W., King, J., Scholz, C.A., Peck, J. The time-transgressive termination of the African humid period. *Nat. Geosci*. 8 http://dx.doi.org/10.1038/NGEO2329 (2015).
5. Street, F.A., Grove, A.T. Environmental and climatic implications of late Quaternary lake-level fluctuations in Africa. *Nature* 261, 385-390 (1976).
6. Gasse, F. Hydrological changes in the African tropics since the last glacial maximum. *Quat. Sci. Rev.* 19, 189-211 (2000).
7. Tierney, J.E., Lewis, S.C., Cook, B.I., LeGrande, A.N., Schmidt, G.A. Model, proxy and isotopic perspectives on the East African humid period. *Earth Planet. Sci. Lett.* 307, 103-112 (2011).
8. Rohling, E.J., Marino, G., Grant, K. Mediterranean climate and oceanography, and the periodic development of anoxic events (sapropels). *Earth-Sci. Rev.* 143, 62-97 (2015).
9. Rossignol-Strick, M. Mediterranean Quaternary sapropels, an immediate response of the African monsoon to variation of insolation. *Palaeogeogr., Palaeoclimatol., Palaeoecol.* 49, 237-263 (1985).

10. Thomson, J., Mercone, D., de Lange, G.J., van Santvoort, P.J.M. Review of recent advances in the interpretation of eastern Mediterranean sapropel S1 from geochemical evidence. *Mar. Geol.* 153, 77-89 (1999).
11. Emeis, K.C. et al. Eastern Mediterranean surface water temperatures and $\delta^{18}O$ composition during deposition of sapropels in the late Quaternary. *Paleoceanography* 18. http://dx.doi.org/10.1029/2000PA000617 (2003).
12. Grant, K.M., Grimm, R., Mikolajewicz, U., Ziegler, M., Rohling, E.J. The timing of Mediterranean sapropel deposition relative to insolation, sea-level and African monsoon changes. *Quat. Sci. Rev.* 140, 125-141. (2016).
13. Lourens, L.J., Wehausen, R., Brumsack, H.J. Geological constraints on tidal dissipation and dynamical ellipticity of the Earth over the past three million years. *Nature* 409, 1029-1033 (2001).
14. Martinez-Boti. M.A. et al. Plio-Pleistocene climate sensitivity evaluated using high-resolution CO_2 records. *Nature* 518, 49-53 (2015).
15. Grant, K.M. et al. A 3 million year index for North African humidity/aridity and the implication of potential pan-African Humid periods. *Quat. Sci. Rev.* 171, 100-118 (2017).
16. Rohling, E.J. et al. Sea-level and deep-sea-temperature variability over the past 5.3 million years. *Nature* 508, 477-482 (2014).
17. Rodriguez-Sanz, L. et al. Penultimate deglacial warming across the Mediterranean Sea revealed by clumped isotopes in foraminifera. *Sci. Rep.* 7: 16572 (2017).
18. Amies, J.D., Rohling, E.J., Grant, K.M., Rodriguez-Sanz, L., Marino, G. Quantification of African Monsoon runoff during last interglacial sapropel S5. *Paleoceanogr. Paleoclimatol.* 34, 1487-1516 (2019).
19. Wu, J., Filippidi, A., Davies, G.R., de Lange, G.J. Riverine supply to the eastern Mediterranean during last interglacial sapropel S5 formation: A basin-wide perspective. *Chem. Geol.* 485, 74-89 (2018).
20. Nicholson, S.E. A review of climate dynamics and climate variability in Eastern Africa. In: Johnson, T.C., Odada, E.O. (Eds.), The Limnology, Climatology and Paleoclimatology of the East African Lakes. Gordon and Breach, Amsterdam, 25-56 (1996).
21. Rohling, E.J. et al. African monsoon variability during the previous interglacial maximum. *Earth Planet. Sci. Lett.* 202, 61-75 (2002).
22. Osborne, A.H. et al. A humid corridor across the Sahara for the migration "Out of Africa" of early modern humans 120,000 years ago. *Proc. Natl. Acad. Sci. U.S.A.* 105, 16444-16447 (2008).
23. Singarayer, J.S., Burrough, S.L. Interhemispheric dynamics of the African rainbelt during the late Quaternary. *Quat. Sci. Rev.* 124, 48-67 (2015).
24. Ruddiman, T.F., Janecek, T.R. Plio-Pleistocene biogenic and terrigenous fluxes at equatorial Atlantic sites 662, 663, and 664. *Proc. ODP Sci. Res.* 108, 211-240 (1989).
25. deMenocal, P.B. Plio-Pleistocene African climate. *Science* 270, 53-59(1995).
26. Larrasoaña, J.C., Roberts, A.P., Rohling, E.J., Winklhofer, M., Wehausen, R. Three million years of monsoon variability over the northern Sahara. *Clim. Dyn.* 21, 689-698 (2003).
27. Trauth, M.H., Larrasoaña, J.C., Mudelsee, M. Trends, rhythms and events in Plio-Pleistocene African climate. *Quat. Sci. Rev.* 28, 399-411 (2009).
28. Vallé, F., Westerhold, T., Dupont, L.M. Orbital‐driven environmental changes recorded at ODP Site 959 (eastern equatorial Atlantic) from the Late Miocene to the Early Pleistocene. *Int. J. Earth Sci.* 106, 1161-1174 (2017).
29. Emeis, K.C., Sakamoto, T., Wehausen, R., Brumsack, H.J. The sapropel record of the eastern Mediterranean Sea — results of Ocean Drilling Program Leg 160. *Palaeogeogr. Palaeoclimatol. Palaeoecol.* 158, 371-395 (2000).
30. Casford. J.S.L. et al. A dynamic concept for eastern Mediterranean circulation and oxygenation during sapropel formation. *Palaeogeogr., Palaeoclimatol., Palaeoecol.* 190, 103-119 (2003).
31. Williams, M.A.J. et al. Causal links between Nile floods and eastern Mediterranean sapropel formation during the past 125 kyr confirmed by OSL and radiocarbon dating of Blue and White Nile sediments. *Quat. Sci. Rev.* 130, 89-108 (2015).
32. Leroy, S., Dupont, L. Development of vegetation and continental aridity in northwestern Africa during the Late Pliocene: the pollen record of ODP Site 658. *Palaeogeogr., Palaeoclimatol., Palaeoecol.* 109, 295-316 (1994).

33. Salzmann, U., Haywood, A.M., Lunt, D.J., Valdes, P.J., Hill, D.J. A new global biome reconstruction and data-model comparison for the Middle Pliocene. *Global Ecol. Biogeogr.* 17, 432-447 (2008).
34. Colleoni, F., Cherchi, A., Masina, S., Brierley, C.M. Impact of global SST gradients on the Mediterranean runoff changes across the Plio-Pleistocene transition. *Paleoceanography* 30, 751-767 (2015).
35. de Boer, M., Peters, M., Lourens, L.J. The transient impact of the African monsoon on Plio-Pleistocene Mediterranean sediments. *Clim. Past* 17, 331-344 (2021).
36. Kuechler, R.R., Dupont, L.M., Schefus, E. Hybrid insolation forcing of Pliocene monsoon dynamics in West Africa. *Clim. Past* 14, 73-84 (2018).
37. Yost, C.L. et al. Phytoliths, pollen, and microcharcoal from the Baringo Basin, Kenya reveal savanna dynamics during the Plio-Pleistocene transition. *Palaeogeogr., Palaeoclimatol., Palaeoecol.* In press, https://doi.org/10.1016/j.palaeo.2020.109779 (2020).
38. Liddy, H.M., Feakins, S.J., Tierney, J.E. Cooling and drying in northeast Africa across the Pliocene. *Earth Planet. Sci. Lett.* 449, 430-438, (2016).
39. Zhang, Z. et al. Aridification of the Sahara desert caused by Tethys Sea shrinkage during the late Miocene. *Nature* 513, 401-404 (2014).
40. Said, R. The Geological Evolution of the River Nile. Springer-Verlag, New York (1981).
41. Abdelsalam, M.G. The Nile's journey through space and time: a geological perspective. *Earth-Sci. Rev.* 177, 742-773 (2018).
42. Sagy, Y., Dror, O., Gardosh, M., Reshef, M. The origin of the Pliocene to recent succession in the Levant basin and its depositional pattern, new insight on source to sink system. *Mar. Petrol. Geol.* 120, 104540 (2020).
43. Williams, M. River sediments. *Phil. Trans. R. Soc. Lond. A* 370, 2093-2122 (2012).
44. Hely, C. et al. Sensitivity of African biomes to changes in the precipitation regime. *Glob. Ecol. Biogeogr.* 15, 258-270 (2006).
45. Gritti, E.S. et al. Simulated effects of a seasonal precipitation change on the vegetation in tropical Africa. *Clim. Past* 6, 169-178 (2010).
46. Chen, W. et al. Feedbacks of soil properties on vegetation during the Green Sahara period. *Quat. Sci. Rev.* 240, 106389 (2020).
47. Lisiecki, L.E., Raymo, M.E. A Pliocene-Pleistocene stack of 57 globally distributed benthic $\delta^{18}O$ records. *Paleoceanography* 20, PA1003, doi:10.1029/2004PA001071 (2005).
48. Mudelsee, M., Raymo, M.E. Slow dynamics of the Northern Hemisphere glaciation. *Paleoceanography* 20, PA4022, doi:10.1029/2005PA001153 (2005).
49. Lawrence, K., Sosdian, S., White, H., Rosenthal, Y. North Atlantic climate evolution through the Plio-Pleistocene climate transitions. *Earth Planet. Sci. Lett.* 300, 329-342 (2010).
50. Herbert, T.D. et al. Late Miocene global cooling and the rise of modern ecosystems. *Nat. Geosci.* 9, 843-847 (2016).
51. Passchier, S. Linkages between East Antarctic Ice Sheet extent and Southern Ocean temperatures based on a Pliocene high-resolution record of ice-rafted debris off Prydz Bay, East Antarctica. *Paleoceanography* 26, PA4204, doi:10.1029/2010PA002061 (2011).
52. Su, Q. et al. Central Asian drying at 3.3 Ma linked to tropical forcing? *Geophys. Res. Lett.* 46, 10,561-10,567 (2019).
53. van Hinsbergen, D.J.J. et al. Orogenic architecture of the Mediterranean region and kinematic reconstruction of its tectonic evolution since the Triassic. *Gondwana Res*. 81, 79-229 (2020).
54. Duermeijer, C.E., Langereis, C.G., Astronomical dating of a tectonic rotation on Sicily and consequences for the timing and extent of a middle Pliocene deformation phase. *Tectonophysics* 298, 243-258 (1998).
55. Oldow, J.S., Channell, J.E.T., Catalano, R., D'Argenio, B. Contemporaneous thrusting and large-scale rotations in the western Sicilian fold and thrust belt. *Tectonics* 9, 661-681 (1990).
56. Catalano, R., Di Stefano, P., Sulli, A., Vitale, F.P. Paleogeography and structure of the central Mediterranean: Sicily and its offshore area. *Tectonophysics* 260, 291-323 (1996).
57. Grimm, R. et al. Late glacial initiation of Holocene eastern Mediterranean sapropel formation. *Nat. Commun.* 6, 7099, doi: 10.1038/ncomms8099 (2015).
58. Planq, J. et al. Multi-proxy constraints on sapropel formation during the late Pliocene of central Mediterranean (southwest Sicily). *Earth Planet. Sci. Lett.* 420, 30-44 (2015).

59. Athanasiou, M. et al. Sea surface temperatures and environmental conditions during the "warm Pliocene" interval (~4.1–3.2 Ma) in the Eastern Mediterranean (Cyprus). *Glob. Planet. Change* 150, 46-57 (2017).
60. Nijenhuis, I.A., Becker, J., De Lange, G.J. Geochemistry of coeval marine sediments in Mediterranean ODP cores and a land section: implications for sapropel formation models. *Palaeogeogr., Palaeoclimatol., Palaeoecol.* 165, 97-112 (2001).
61. Passier, H.F. et al. Sulphidic Mediterranean surface waters during Pliocene sapropel formation. *Nature* 397, 146-149 (1999).
62. Nijenhuis, I.A., De Lange, G.J., 2000. Geochemical constraints on Pliocene sapropel formation in the eastern Mediterranean. *Mar. Geol.* 163, 41-63. (2000).
63. Castradori, D. Calcareous nannofossils in the basal Zanclean of the Eastern Mediterranean Sea: remarks on paleoceanography and sapropel formation. *Proc. ODP Sci. Res.* 160, 113-124 (1998).
64. Sgarella, F., Di Donato, V., Sprovieri. R. Benthic foraminiferal assemblage turnover during intensification of the Northern Hemisphere glaciation in the Piacenzian Punta Piccola section (Southern Italy). *Palaeogeogr., Palaeoclimatol., Palaeoecol.* 333-334, 59-74 (2012).
65. Haywood, B.W., Sabaa, A.T., Kawagata, S., Grenfell, H.R. The Early Pliocene re-colonisation of the deep Mediterranean Sea by benthic foraminifera and their pulsed Late Pliocene–Middle Pleistocene decline. *Mar. Micropaleontol.* 71, 97-112 (2009).
66. Khélifi, N. et al. A major and long-term Pliocene intensification of the Mediterranean outflow, 3.5–3.3 Ma ago. *Geology* 37, 811-814 (2009).
67. Hernandez-Molina, F.J. et al. Onset of Mediterranean outflow into the North Atlantic. *Science* 344, 6189 (2014).
68. Tzanova, A., Herbert, T.D. Regional and global significance of Pliocene sea surface temperatures from the Gulf of Cadiz (Site U1387) and the Mediterranean. *Glob. Planet. Change* 133, 371-377 (2015).
69. Westerhold, T. et al. An astronomically dated record of Earth's climate and its predictability over the last 66 million years. *Science* 369, 1383-1387 (2020).
70. Hennekam, R. et al. Early-warning signals for marine anoxic events. *Geophys. Res. Lett.* 47, e2020GL089183, https://doi.org/10.1029/2020GL089183 (2020).
71. Lupien, R.L. et al. Vegetation change in the Baringo Basin, East Africa across the onset of Northern Hemisphere glaciation 3.3–2.6 Ma. *Palaeogeogr., Palaeoclimatol., Palaeoecol.* In press, https://doi.org/10.1016/j.palaeo.2019.109426 (2019).
72. Knorr, W., Schnitzler, K.-G. Enhanced albedo feedback in North Africa from possible combined vegetation and soil-formation processes. *Clim. Dyn.* 26, 55-63 (2006).
73. Tierney, J.E., Pausata, F.S.R., deMenocal, P.B. Rainfall regimes of the Green Sahara. *Sci. Adv.* 3, e1601503 (2017).
74. Rohling, E.J. et al. Sea-level and deep-sea temperature reconstructions suggest quasi-stable states and critical transitions over the past 40 million years. *Sci. Adv. in press* (2021).

Figures

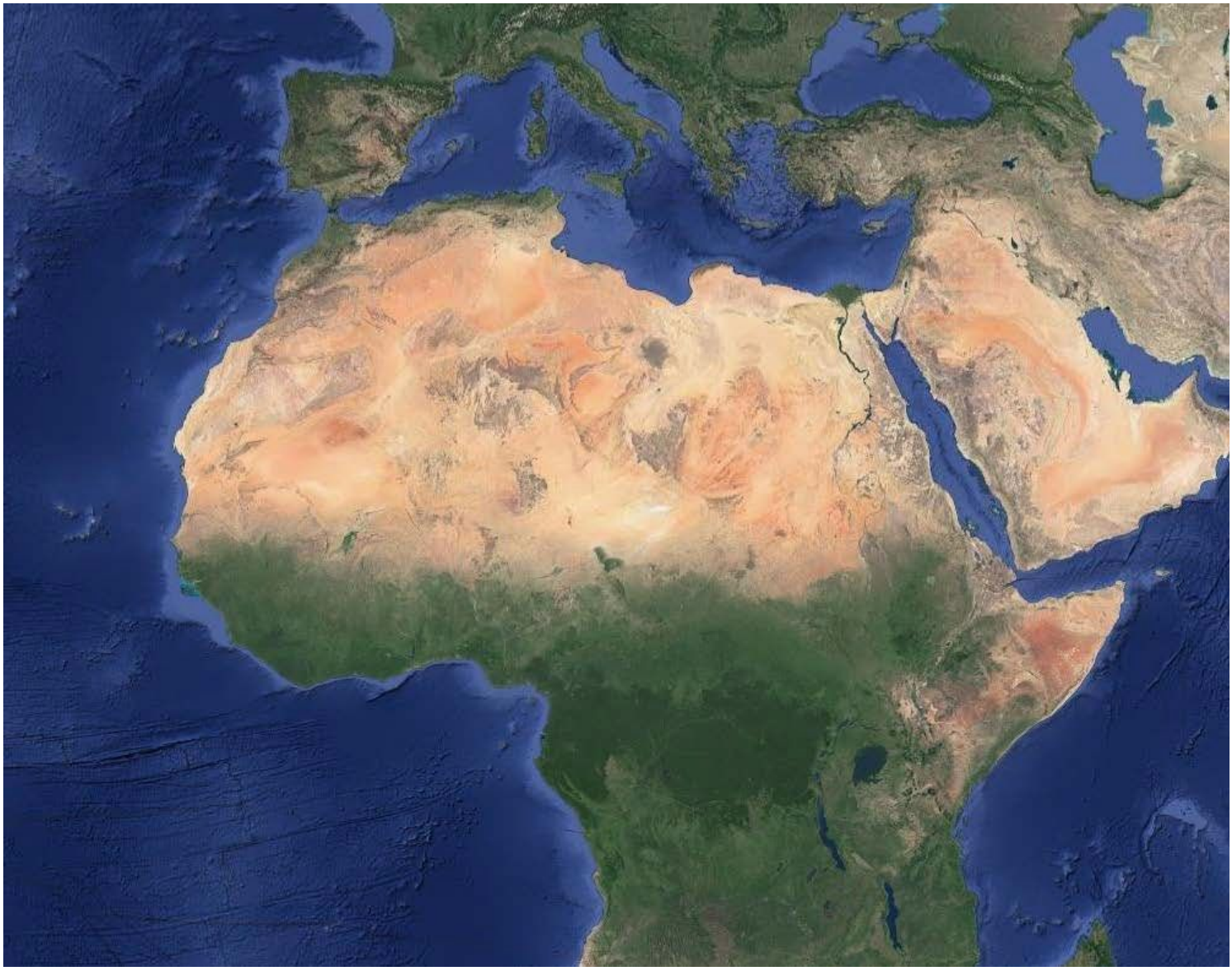

Figure 1

Locations of sites discussed in this study. Eastern Mediterranean sites are from Ocean Drilling Program (ODP) Leg 160ref.29.

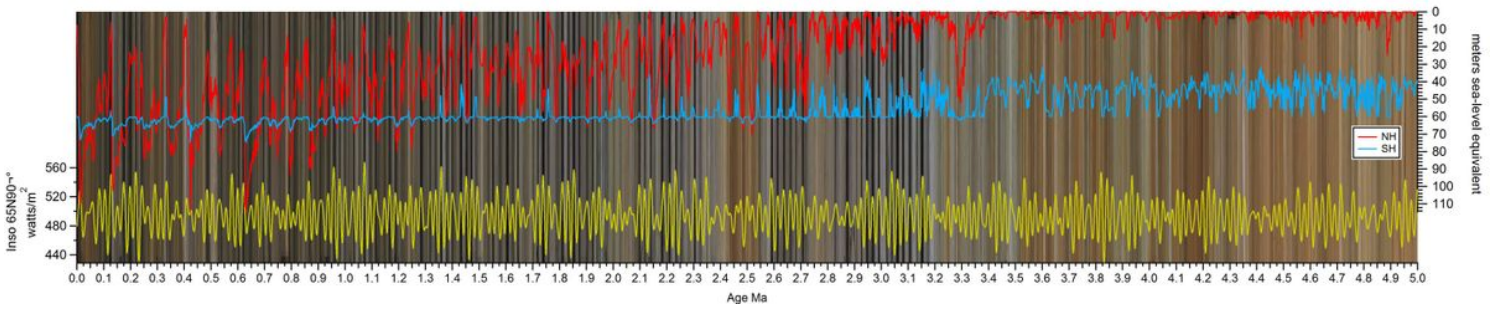

Figure 2

ODP967 composite core image. Northern and Southern Hemisphere ice-volume changes (NH, red; SH, blue), in equivalent sea-level fall, and June 21 insolation at 65N (yellow) illustrate timing relationships between climate forcing and lithology.

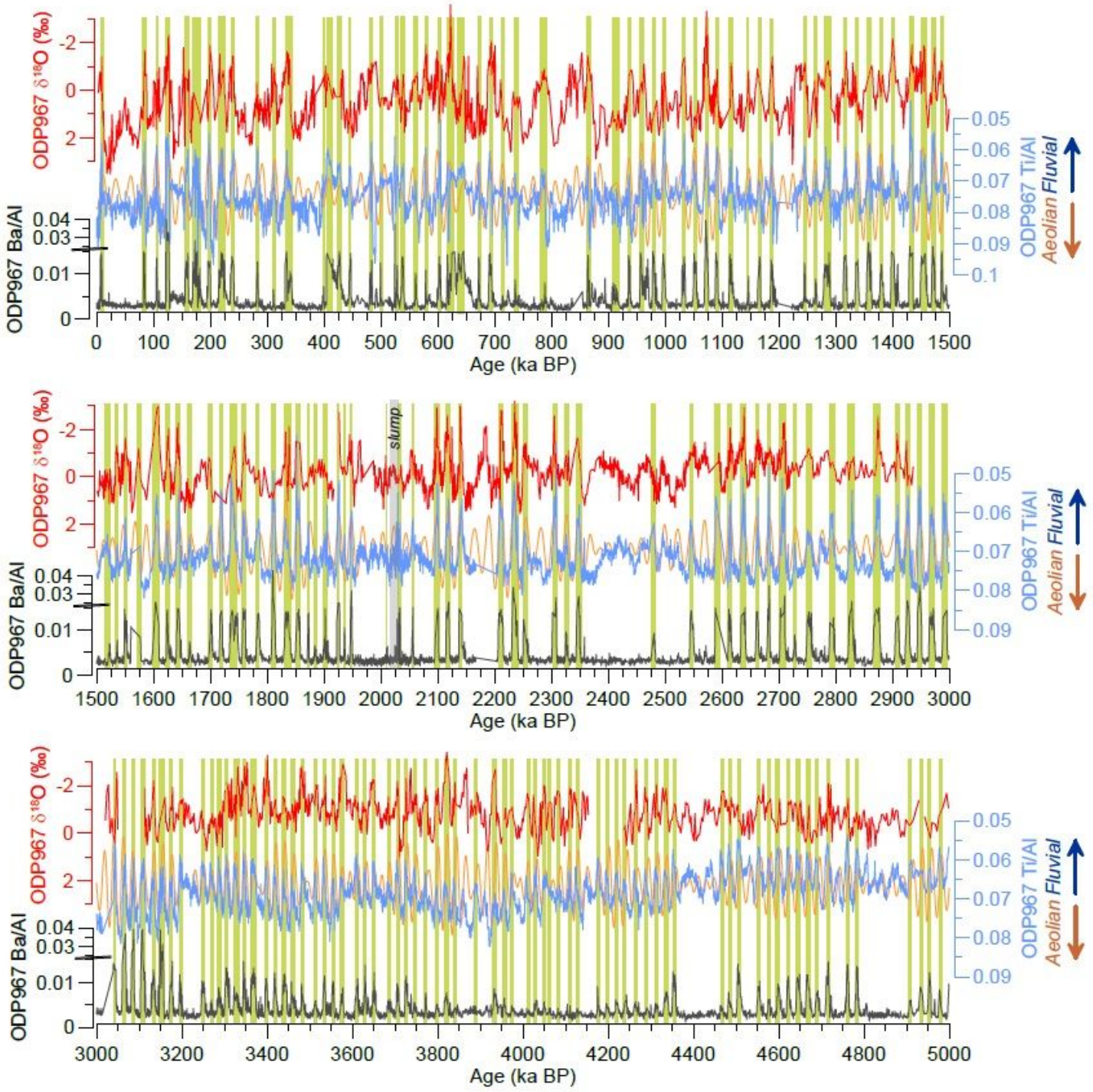

Figure 3

Site 967 records of planktic foraminifera (G. ruber) 18O (red), Ti/Al (blue), and Ba/Al (grey) for time intervals 0-1.5 Myr ago (top), 1.5-3 Myr ago (middle) and 3-5 Myr ago (bottom), with time in kiloyears

before Present. Upward peaks correspond to precession minima (orange) and Green Sahara Periods (green shading). (See Supplementary Fig. S2 for detail over a selected interval).

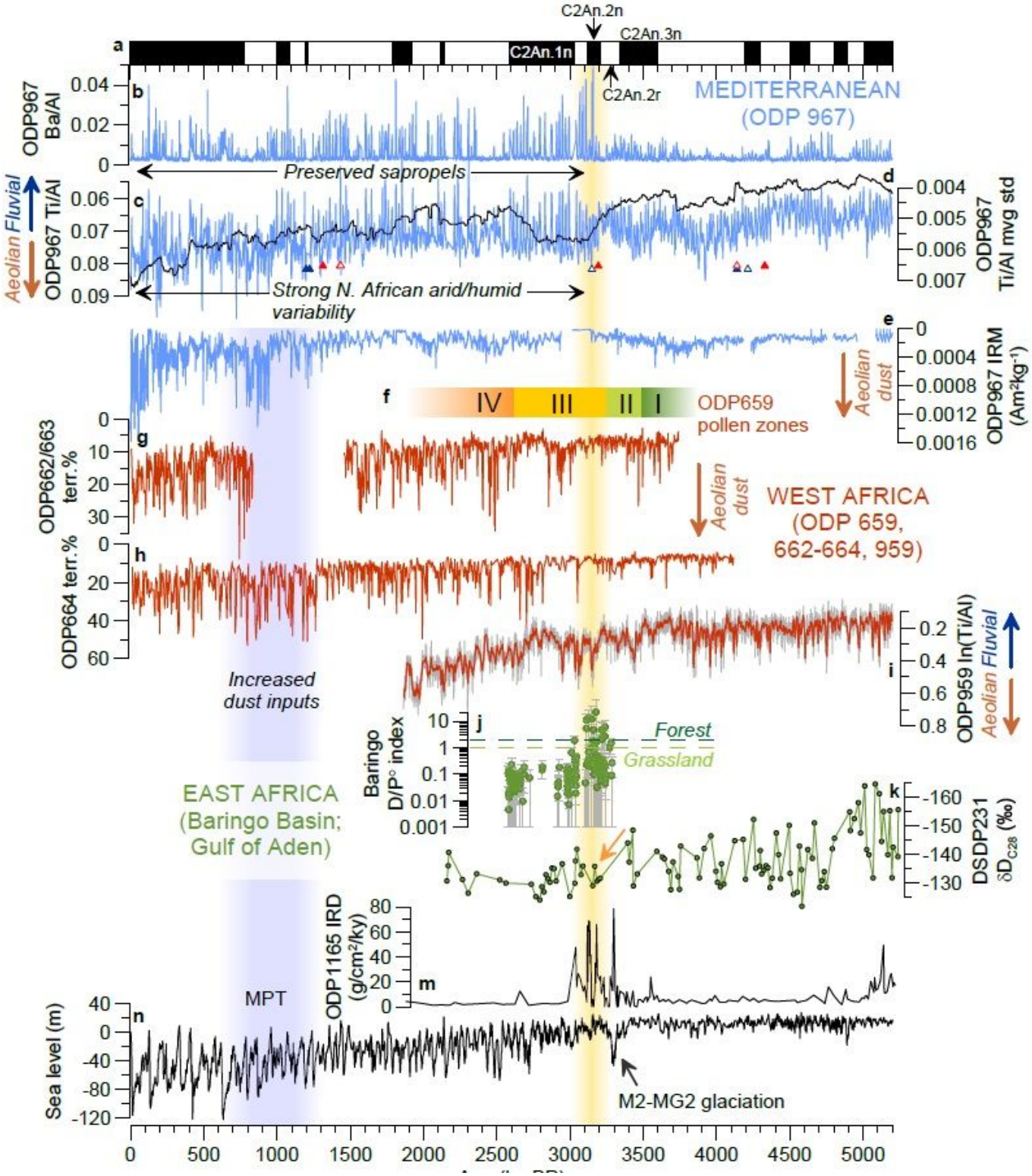

Figure 4

Chronological and environmental context for ODP967 geochemical shift at 3.2 Ma (see Fig. 1 for site locations). a) Tectonic event around Sicily in Chron 2An.2n; b-e) ODP967 Ba/Al, Ti/Al, 400-kyr moving standard deviation of Ti/Al (black), and magnetic dust proxy (IRM900@120mT) (this study). Change-

points in (c) are based on changes in the mean (red) and standard deviation (blue) of the Ti/Al time-series (closed triangles) and Ti/Al residuals (open triangles) after removing low-frequency (140-1200 kyr) variability; f) pollen zones from ODP Site 659ref.32 (green = more humid; yellow/orange = increasing aridity and humid/arid variability); g-h) aeolian dust records from offshore West Africa24,25; i) ODP Site 959 Ti/Al (grey)28 with 11-point running average (red); j) tree index based on pollen from Baringo Basin core BTB13, with 95% confidence intervals37 (downward bars limited to y-axis); k) DSDP Site 231 leaf wax δD with inferred shift to more aridity at 3.3-3.0 Maref.38; m) ODP Site 1165 ice-rafted debris (IRD) fluxes51; n) global sea-level reconstruction74 based on benthic δ18O (ref. 69). All records are plotted on their original chronology. Vertical shading denotes the Mid-Pleistocene Transition (MPT; grey) and geochemical shift at ODP967 (yellow).

Supplementary Files

This is a list of supplementary files associated with this preprint. Click to download.

- MethodsNGeo.docx
- SupplementaryFigures.pdf